ZooKeys 1215: 139–149 (2024)
DOI: 10.3897/zookeys.1215.129623

Research Article

Distribution extension of a vent scale worm *Branchinotogluma bipapillata* (Polychaeta, Polynoidae) in the Indian Ocean

Won-Kyung Lee[1,2], Se-Joo Kim[1,3]

1 *Division of Biomedical Research, Korea Research Institute Bioscience and Biotechnology, Daejeon 34141, Republic of Korea*
2 *Division of EcoScience, Ewha Womans University, Seoul 03760, Republic of Korea*
3 *KRIBB School, University of Science and Technology, Daejeon, 34113, Republic of Korea*
Corresponding author: Se-Joo Kim (biosejoo@kribb.re.kr)

Abstract

Branchinotogluma Pettibone, 1985 is the most species-rich genus within the subfamily Lepidonotopodinae Pettibone, 1983, comprising 18 valid species from chemosynthesis-based ecosystems in the Pacific and Indian Oceans. Here, we report a new distributional record of *Branchinotogluma bipapillata* Zhou, Wang, Zhang & Wang, 2018, at the hydrothermal vent sites on the northern Central Indian Ridge (nCIR). This record represents the northernmost occurrence of *B. bipapillata* in the Indian Ocean. We conducted a comparative study of the nCIR population and other documented populations using distributional information, morphological traits, and genetic markers (two mitochondrial [*COI*, *16S* rRNA] and one nuclear [*18S* rRNA] genes). While most morphological characters of *B. bipapillata* were consistent with those found in the Southwest Indian Ridge (SWIR), variations were noted in the segment with the last branchiae. Molecular data revealed that all populations of *B. bipapillata* form a single clade, indicating a wide distribution from the SWIR to nCIR, covering ~4,000 km across various ridges in the Indian Ocean. This study presents extensive distribution of a vent species with well-connected populations throughout the Indian Ocean, distinguishing it from many other vent species affected by the dispersal barrier in the Indian Ocean.

Key words: *16S* rRNA, *18S* rRNA, *CO1*, deep-sea, hydrothermal vent, northern Central Indian Ridge, polynoids

OPEN ACCESS

Academic editor: Andrew Davinack
Received: 13 June 2024
Accepted: 2 September 2024
Published: 14 October 2024

ZooBank: https://zoobank.org/4A593809-AE76-458F-B085-0D34B29105CC

Citation: Lee W-K, Kim S-J (2024) Distribution extension of a vent scale worm *Branchinotogluma bipapillata* (Polychaeta, Polynoidae) in the Indian Ocean. ZooKeys 1215: 139–149. https://doi.org/10.3897/zookeys.1215.129623

Copyright: © Won-Kyung Lee & Se-Joo Kim. This is an open access article distributed under terms of the Creative Commons Attribution License (Attribution 4.0 International – CC BY 4.0).

Introduction

The subfamily Lepidonotopodinae Pettibone, 1983 consists of scale worms endemic to chemosynthesis-based ecosystems (Wu et al. 2023). Currently, seven species from the Indian Ocean are identified within this subfamily: three *Branchinotogluma*, two *Branchipolynoe*, and two *Levensteiniella* (Han et al. 2023). *Branchinotogluma* Pettibone, 1985, the most species-rich genus in the subfamily, comprises 18 species found in the Pacific and Indian Oceans (Han et al. 2023). Specifically, three *Branchinotogluma* species are distributed across different ridge systems in the Indian Ocean: *B. bipapillata* Zhou et al., 2018 in the Southwest Indian Ridge (SWIR) and southern Central Indian Ridge (sCIR), *B. jiaolongae* Han et al., 2023 in the SWIR and Carlsberg Ridge (CR), and *B. kaireiensis* Han et al., 2023 in the sCIR and CR (Zhou et al. 2018, 2022; Han et al. 2023).

Since the initial discovery of vent fields in the Indian Ocean in 2000, the Rodriguez Triple Junction, which links the SWIR, CIR, and Southeast Indian Ridge, was assumed to be a dispersal barrier for vent species within the Indian Ocean (Gamo et al. 2001; Chen et al. 2015). However, with the discovery of more vent fields and associated fauna, it now appears that the primary dispersal barriers lie within the ridge system itself, mainly due to ridge offsets, rather than between different ridge systems (Sun et al. 2020). For instance, the vent crab *Austinograea rodriguezensis* Tsuchida & Hashimoto, 2002 was absent from the southern SWIR (sSWIR) but was found in the northern SWIR (nSWIR) and showed panmixia with populations from other ridges like the sCIR. Similarly, the distribution of the hairy snail *Alviniconcha* species complex shows connectivity between different ridges, northern CIR (nCIR) and CR, but subdivisions between the sCIR and nCIR on the same CIR (Sun et al. 2020; Jang et al. 2023).

While *B. bipapillata* has been reported from vent fields on two ridge systems, the SWIR and CIR, morphological and genetic studies were previously only conducted on specimens from the sSWIR. In this study, we collected *Branchinotogluma* species from hydrothermal vent fields on the nCIR and compared morphological and molecular data with those from vent fields on the sSWIR.

Materials and methods

Specimens of *Branchinotogluma* were collected from hydrothermal vents in the nCIR during the 2023 KIOST expedition aboard the R/V *Isabu* (Fig. 1, Table 1) using a suction sampler and scoop mounted on the ROV ROPOS (Canadian Scientific Submersible Facility). Upon collection, a piece of elytron or parapodium from each specimen was dissected and preserved in 99% ethanol for molecular analysis. The entire body of the specimens was preserved in either 10% neutral buffered formalin or 70% ethanol for morphological studies.

For determination of morphological characters, all specimens were examined under a stereomicroscope (Stemi 508; Carl Zeiss, Germany). Specimen photographs were captured using a color camera (Axiocam 208 color; Carl Zeiss, Germany) and a DSLR camera (EOS 5D Mark IV; Canon, Tokyo, Japan). Images were processed with ZEN 3.3 blue edition (Carl Zeiss, Germany) and Helicon Focus software (Helicon Soft Ltd., Kharkov, Ukraine), and further edited using Adobe Photoshop 2022 (Adobe, San Jose, CA, USA). Specimen morphology was recorded following characters and states listed in Zhou et al. (2018).

A small piece of elytron or parapodium was used for total genomic DNA extraction using the AccuPrep® Genomic DNA Extraction Kit (Bioneer, Daejeon, South Korea), following the manufacturer's instructions. Partial cytochrome c oxidase subunit 1 (*CO1*) and *18S* rRNA (*18S*) sequences were amplified following the protocols in Lee et al. (2021) and Jimi et al. (2021), respectively. For *16S* rRNA (*16S*), the primers 16SA (5'-CGCCGTTTATCAAAAACAT-3') and 16Sbr (5'-CCGGTYTGAACTCAGATCAYG-3') (Palumbi et al. 1991; Palumbi 1996) were used. Polymerase chain reaction (PCR) was conducted using a SimpliAmp™ Thermal Cycler (Applied Biosystems, Life technologies) under the following conditions: initial denaturation at 94 °C for 2 min; 5 cycles at 95 °C for 10 s, 42 °C for 30 s, and 72 °C for 60 s; 35 cycles at 95 °C for 10 s, 48 °C for 30 s, and 72 °C for 60 s; with a final extension at 72 °C for 2 min. PCR products were sent to Macrogen (Seoul, Korea) for Sanger sequencing.

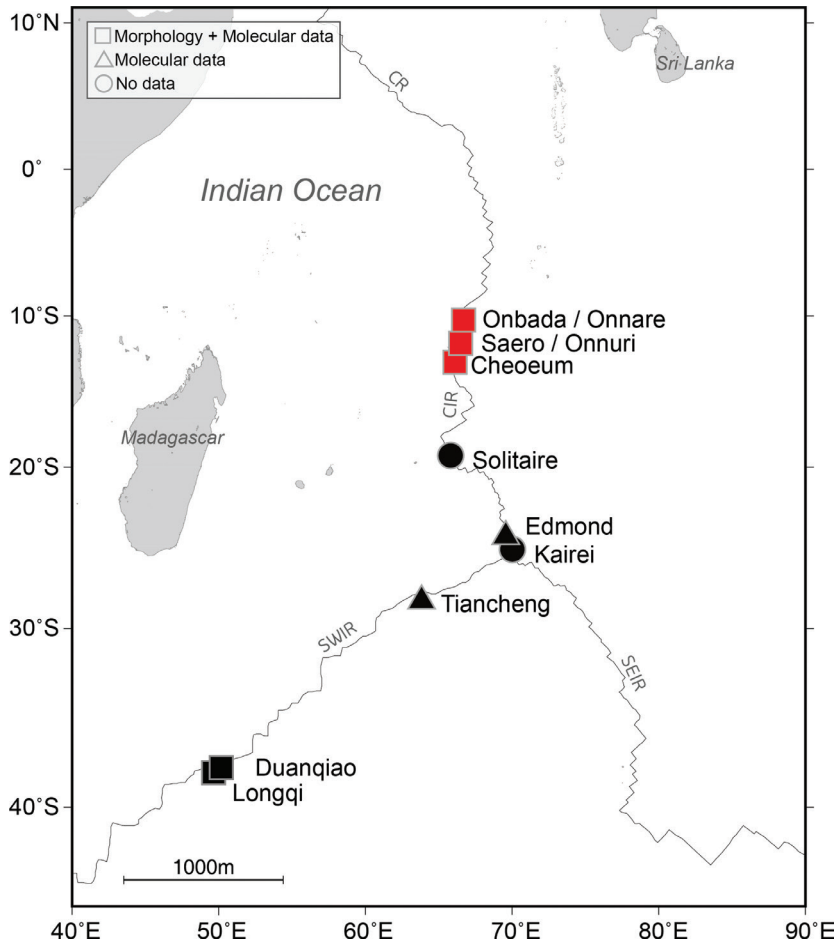

Figure 1. Map displaying the geographic distribution of *Branchinotogluma bipapillata* in the Indian Ocean. Red indicates sampling locations from this study and black indicates records of *B. bipapillata* from previous studies. Some closely situated sampling sites (< 10 km apart, such as Onbada and Onnare, Saero and Onnuri) are marked with a single square.

Table 1. Sampling information of newly obtained *Branchinotogluma bipapillata* specimens from the nCIR and their GenBank accession numbers sequenced in this study.

Voucher	Sampling site	Latitude (S), Longitude (E)	Depth (m)	GenBank Accession Numbers		
				CO1	*16S*	*18S*
KRIBB310101–KRIBB310102	Cheoeum	12°37.1'S, 66°7.6'E	3018	PP600168–PP600169	PP600150–PP600151	PP600184–PP600185
KRIBB310103–KRIBB310107	Onnuri	11°24.9'S, 66°25.4'E	2009	PP600170–PP600174	PP600152–PP600156	PP600186–PP600190
KRIBB310108–KRIBB310110	Onnare	9°47.4'S, 66°41.9'E	2993	PP600175–PP600177	PP600157–PP600159	PP600191–PP600193
KRIBB310111–KRIBB310112	Onbada	9°48.9'S, 66°40.6'E	2563	PP600178–PP600179	PP600160–PP600161	PP600194–PP600195
KRIBB310113–KRIBB310116	Saero	11°19.7'S, 66°26.9'E	3256	PP600180–PP600183	PP600162–PP600165	PP600196–PP600199

New sequences were aligned with those of other Lepidonotopodinae species from GenBank (Suppl. material 1: table S1) using Geneious Prime ver. 2023.0.1 (Biomatters, Auckland, New Zealand). Sequence divergence for the *CO1* and *16S* genes was calculated using the *p*-distance method in MEGA11 (Tamura et al. 2021). For phylogenetic analysis, the three genes were concatenated using

Geneious Prime. The best evolutionary model, GTR+I+G, was selected using jModelTest ver. 2.1.8 (Darriba et al. 2012). The phylogenetic tree was constructed using the maximum-likelihood method with raxmlGUI 2.0 (Edler et al. 2021).

All specimens used in this study are deposited at the Korea Research Institute of Bioscience and Biotechnology.

Results

Family Polynoidae Kinberg, 1856
Subfamily Lepidonotopodinae Pettibone, 1983

Genus *Branchinotogluma* Pettibone, 1985

Branchinotogluma bipapillata Zhou, Wang, Zhang & Wang, 2018: 528–533, figs 1–7; table 1.

Material examined. Indian Ocean • 2 ♂; Cheoeum; 12°37.1'S, 66°07.6'E; depth 3018 m; 28 Mar. 2023; W-K Lee leg.; hydrothermal vent; GenBank: PP600168–PP600169; KRIBB310101 to KRIBB310102 • 2 ♂, 2 ♀, 1 undetermined; Onnuri; 11°24.9'S, 66°25.4'E; depth 2009 m; 1–2 Apr. 2023; W-K Lee leg.; hydrothermal vent; GenBank: PP600170– PP600174; KRIBB310103 to KRIBB310107 • 1 ♀, 2 undetermined; Onnare; 9°47.4'S, 66°41.9'E; depth 2993 m; 3 Apr. 2023; W-K Lee leg.; hydrothermal vent; GenBank: PP600175– PP600177; KRIBB310108 to KRIBB310110 • 1 ♂, 1 ♀; Onbada; 9°48.9'S, 66°40.6'E; depth 2563 m; 4 Apr. 2023; W-K Lee leg.; hydrothermal vent; GenBank: PP600178– PP600179; KRIBB310111 to KRIBB310112 • 2 ♂, 2 ♀; Saero; 11°19.7'S, 66°26.9'E; depth 3256 m; 7 Apr. 2023; W-K Lee leg.; hydrothermal vent; GenBank: PP600180– PP600183; KRIBB310113 to KRIBB310116.

Description. Specimens relatively well preserved, with 21 segments, 12.0–51.0 mm in length and 5.0–16.6 mm in width. Body shape fusiform, tapered anteriorly and posteriorly (Fig. 2A, B, Table 2). Pairs of elytra on elytrophores on segments 2, 4, 5, 7, 9, 11, 13, 15, 17, and 19; elytra oval to subreniform, white, slightly transparent, with a smooth surface (Fig. 2C–E). Dorsal cirri on segments 3, 6, 8, 10, 12, 14, 16, 18, 20, and 21, extending beyond the tips of neurochaetae. Branchiae arborescent; grouped in two, one at base of the notopodia and another at base of dorsal tubercles or elytrophores; starting from segment 3 and ending between segments 18 or 21 (Table 2).

Prostomium bilobed, triangular anterior lobes with slender frontal filaments (Fig. 2F). Median antennae on anterior notch, with a cylindrical ceratophore and subulate style; palps thick, smooth, and end in subulate tips; lateral antennae and eyes absent (Fig. 2F). Tentacular segment fused to prostomium, with pair of tentacular cirri on each side, and a small acicular lobe at the base of tentaculophore; tentacular cirri slender (Fig. 2F).

First segment not distinct, fused to prostomium. Pharynx with five dorsal and four ventral papillae in one immature individual, but not seen in others (Fig. 2G). Second segment with first pair of elytrophores, ventral cirri, and biramous parapodia. Third segment with ventral cirri and first pair of branchiae. Fourth to last segments with ventral cirri and biramous parapodia. Notopodia smaller than neuropodia; notochaetae stout, few, arranged in radiating bundles; neurochaetae slender, numerous, forming a fan shape (Fig. 2H–K).

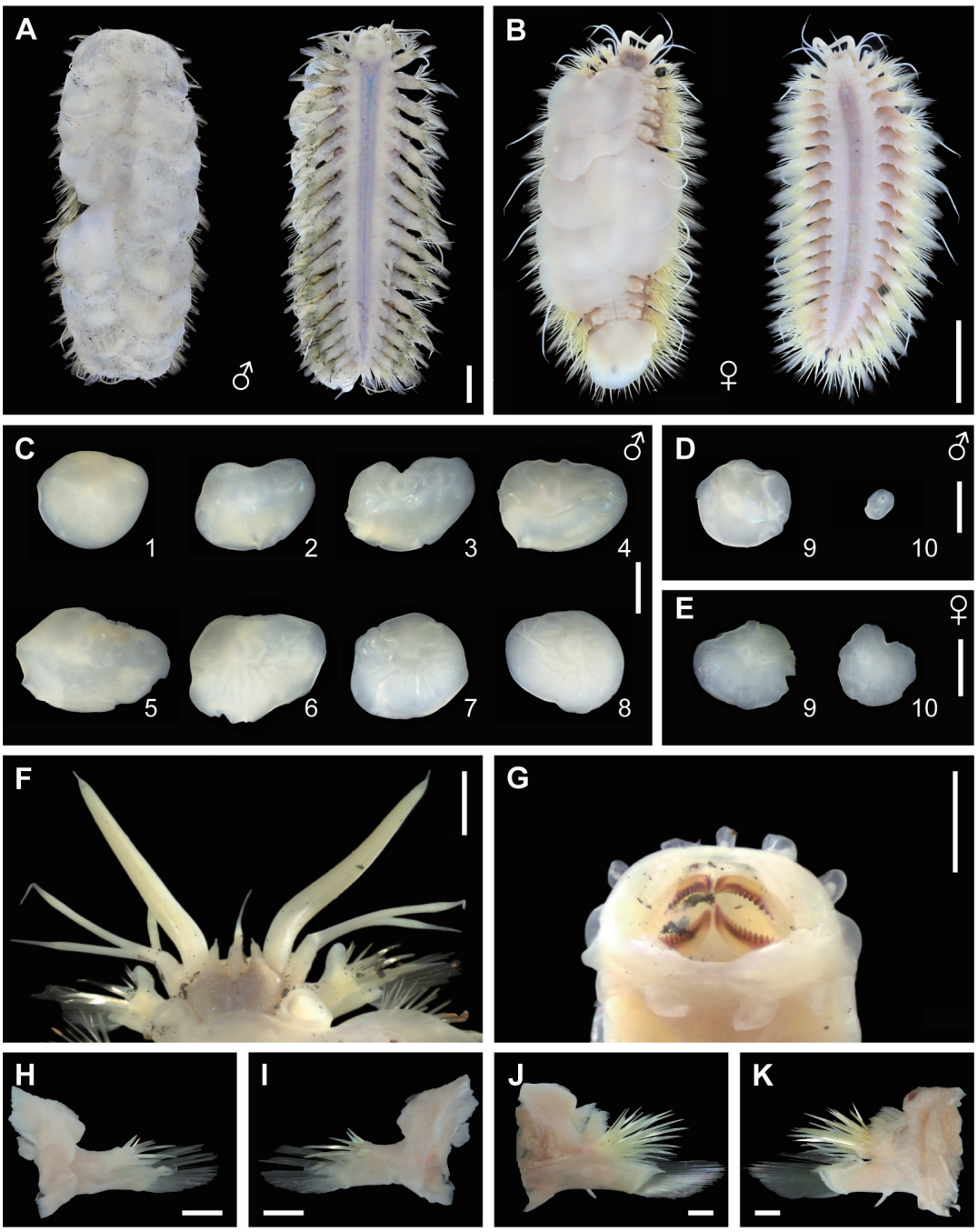

Figure 2. *Branchinotogluma bipapillata* specimens collected from the nCIR **A** dorsal and ventral views of male (KRIBB310116) **B** dorsal and ventral views of female (KRIBB310105) **C** 1st–8th left elytra **D** 9th–10th left elytra of male (KRIBB310103) E 9th–10th left elytra of female (KRIBB310110) **F** head featuring prostomium, palps, tentacular cirri, and first parapodia on segment 2 (KRIBB310112) **G** everted pharynx with dorsal and ventral papillae (KRIBB310108). Anterior and posterior views of left parapodia on (H-I) segment 2 and (J-K) segment 11 (KRIBB310106). Scale bars: 5 mm (**A–E**); 0.5 mm (**F, G**); 1 mm (**H–K**).

Sexual dimorphism evident. In males, posterior segments modified (Fig. 3A) with 10th elytra and elytrophores much smaller than 9th (Figs 2D, 3A, Table 2); ventral papillae present on segments 12–13, long, tapering, with slender tips extending to next segment; ventral lamellae on segments 14–17, round (Fig. 3B). In females, posterior segments not modified (Fig. 3C), with 10th elytra and elytrophores similar to 9th (Figs 2E, 3C, Table 2); ventral papillae present on segments 11–15, short and blunt (Fig. 3D).

Distribution. Indian Ocean (depth 1732–3256 m): Longqi and Duanqiao vent fields on the southern Southwest Indian Ridge; Tiancheng vent field on the northern Southwest Indian Ridge; Edmond vent field on the southern Central Indian Ridge; Onnare, Onbada, Saero, Onnuri, and Cheoeum vent fields on the northern Central Indian Ridge.

Remarks. Comparisons of key morphological characters between the geographically distant populations are present in Table 2. The key characters of the nCIR specimens of *B. bipapillata* largely correspond with those of the SWIR specimens (Zhang et al. 2018). However, the two populations differ in the last segment with branchiae in females (segment 19 in sSWIR compared with segment 18 or 21 in nCIR; Table 2).

Among the 16 specimens from the nCIR population, 10 specimens with body length greater than 20 mm were well-developed in all features indicating adult morphology, while characters of sexual dimorphism were not observed in 6 specimens shorter than 20 mm.

DNA barcoding and phylogenetic analysis. Partial sequences of *CO1*, *16S*, and *18S* were recovered from 16 specimens collected from the nCIR. As shown in Table 1, 48 newly obtained sequences have been deposited in GenBank.

In *CO1*, the mean intra-population variation was 0.56% for nCIR and 0.65% for SWIR, with an inter-population variation of 1.00% (Table 3). In *16S*, the mean intra-population variation was 0.27% for nCIR and 0.33% for SWIR, with an inter-population variation of 0.39%. In *18S*, the mean intra-population variation was 0.01% for nCIR and 0.00% for SWIR, with an inter-population variation of 0.004%.

The interspecific variation between *B. bipapillata* and other congeners ranged from 18.63% to 21.88% in *CO1*, and from 13.11% to 19.08% in *16S* (Suppl. material 1: table S2). In *18S*, the interspecific variation ranged from 1.69% to 3.80%.

Table 2. Morphological comparison of *Branchinotogluma bipapillata* from the nCIR and sSWIR.

Region	Length (mm)	Sex (# of ind.)	Last segment with branchiae	Number of dorsal/ventral papillae on pharynx	9th to 10th elytrophore diatmeter ratio	Reference
nCIR	24.4–48.0	Male (5)	18	Not observed	2.25–2.64	This study
	20.5–51.0	Female (8)	18 or 21		1.08–1.46	
	12.0–17.8	Undetermined (3)	18	5/4*	1.23–1.28	
SWIR	23.3–32.3	Male (1)	18	5/5	N/A	Zhou et al. 2018
		Female (2)	19		N/A	

*Observed in a single specimen (KRIBB310108; Fig. 2G).

Table 3. Sequence divergence (%) among three *Branchinotogluma bipapillata* populations based on partial *CO1* gene (553 bp).

Populations (# of ind.; intra)	nCIR	sCIR	SWIR
nCIR	–		
(16; 0.56)			
sCIR	0.70	–	
(1; NC*)	(0.20–1.18)		
SWIR	1.00	0.47	–
(5; 0.65)	(0.00–1.65)	(0.20–1.19)	

*not calculated.

The maximum likelihood phylogenetic tree, constructed with concatenated sequences of *CO1*, *16S*, and *18S* (Fig. 4), shows the SWIR and nCIR populations of *B. bipapillata* clustering together as a single clade, indicating no significant divergence between populations from different ridges. Within the *Branchinotogluma* genus, *B. bipapillata* is closely related to a clade including *B. kaireiensis*, *B. pettiboneae* Wu et al., 2019, and *B. robusta* Wu et al., 2023.

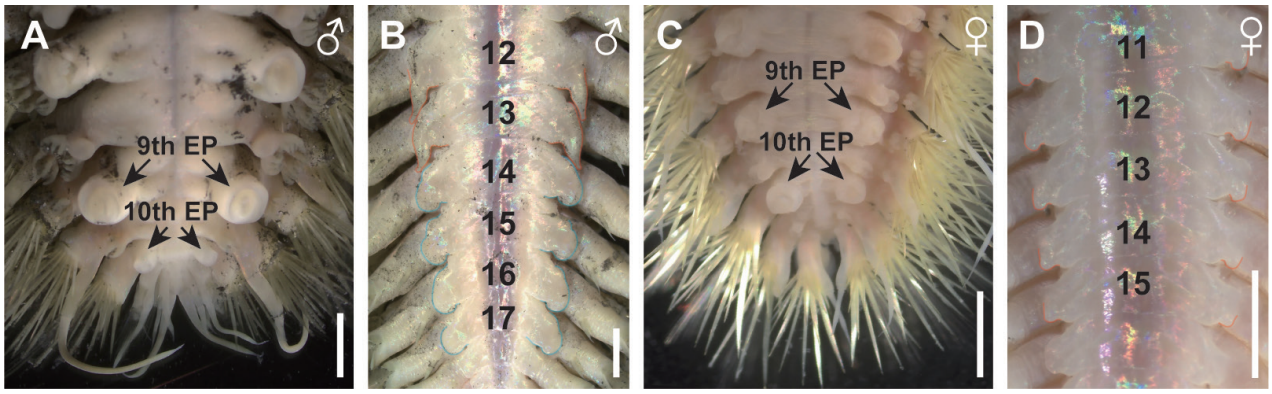

Figure 3. Sexually dimorphic characters of *Branchinotogluma bipapillata* **A** dorsal view of posterior segments **B** ventral view of segments 12–17 of male (KRIBB310116) **C** dorsal view of posterior segments **D** ventral view of segments 11–15 of female (KRIBB310105). Arrows point to 9th and 10th elytrophores (EP) pointed with arrows. Ventral papillae are outlined in red and ventral lamellae in blue. Scale bars: 2 mm (A, C); 1 mm (B, D).

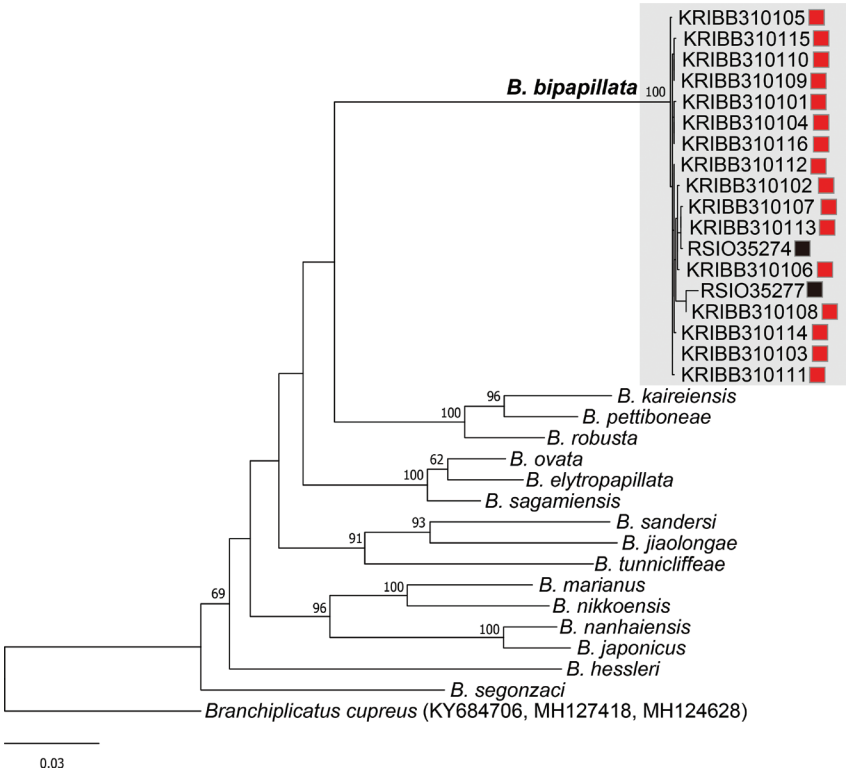

Figure 4. Maximum-likelihood phylogenetic tree of *Branchinotogluma* species based on concatenated sequences of the *CO1*, *16S*, and *18S* genes. *Branchinotogluma bipapillata* species are highlighted with a gray box. Red and black squares represent nCIR and sSWIR populations, respectively. GenBank accession numbers of the *CO1*, *16S* and *18S* genes of the outgroup are noted next to the species names. Maximum-likelihood bootstrap support values > 60 are displayed next to the nodes.

Discussion and conclusion

The vent scale worm *B. bipapillata* is widely distributed in the Indian Ocean, but comprehensive morphological and molecular data are lacking across all deep-sea oceanic ridges, and specimens are rarely reported at each sampling site (Fig. 1; only five specimens of *B. bipapillata* from the SWIR were barcoded with *CO1*, and only two sequences of *16S* and *18S* are available from SWIR specimens). In this study, 16 individuals, including female, male, and immature specimens of *B. bipapillata* from the nCIR were observed, enriching descriptions of features such as all elytra, and improving the molecular description of this species with both nuclear and mitochondrial gene sequences. Key morphological characters, such as the presence of an acicular lobe on the tentaculophore and the position of segmental ventral papillae, showed general congruence between the sSWIR and nCIR populations. Additionally, *CO1* barcode sequences revealed a mean intraspecific variation of 0.72% in *B. bipapillata*, which is within the variation range observed in other *Branchinotogluma* species (0.00–1.05%; Suppl. material 1: table S2).Thus, molecular data on genetic distances within and between populations showed no significant differences, and the phylogenetic analysis revealed a single clade of *B. bipapillata*, with no divergence between populations (Fig. 4, Table 3). Based on these morphological and molecular findings, the southernmost and northernmost populations appear to be well connected, forming a single genetic population with minimal morphological variability.

Other vent endemic species in the Indian Ocean, such as the mussel *Bathymodiolus marisindicus* Hashimoto, 2001, the snail *Chrysomallon squamiferum* Chen et al., 2015, the crab *A. rodriguezensis*, the barnacle *Neolepas marisindica* Watanabe et al., 2018, and the worm *Ophryotrocha jiaolongi* Zhang et al., 2017, all show a wide distribution range on the SWIR and CIR (Sun et al. 2020; Zhou et al. 2022). However, unlike the *B. bipapillata* populations in this study, most of these species exhibit low connectivity between populations, likely due to ridge offsets acting as dispersal barriers between the sSWIR and nSWIR, which do not seem to affect the connectivity of *B. bipapillata* (Sun et al. 2020; Zhou et al. 2022). Although the reproductive and larval development strategies of *B. bipapillata* are not fully understood, observations of other species within the same subfamily suggest that *B. bipapillata* likely have lecithotrophic larvae (Van Dover et al. 1999; Jollivet et al. 2000). This larval type, capable of traveling long distances in oligotrophic deep-sea environments, might partially explain the high connectivity of *B. bipapillata* populations across ~4,000 km of different ridges within the Indian Ocean.

Many studies have considered geological and hydrological features, along with the dispersal abilities of species, to explain the distribution of vent species (Slatkin 1987; Vrijenhoek 2010; Taylor and Roterman 2017; Perez et al. 2021). However, to fully understand the broad geographical distribution of these species, it is also crucial to consider their ability to adapt to diverse vent environments across different ridge systems. To further elucidate the strategies that enable species such as *B. bipapillata* to inhabit separate and geographically distant vent fields with no genetic differentiation, future studies should consider in vitro experiments for culturing as well as transcriptomic and genomic level data of populations.

Acknowledgements

We thank all scientists and crew members of the R/V *Isabu* from KIOST for their support in sampling and data collection.

Additional information

Conflict of interest

The authors have declared that no competing interests exist.

Ethical statement

No ethical statement was reported.

Funding

This work was supported by the Basic Science Research Program of the National Research Foundation of Korea, funded by the Ministry of Education (2021R1I1A2044998), the Korea Institute of Marine Science & Technology Promotion funded by the Ministry of Oceans and Fisheries, Korea (RS-2021-KS211514), and the Korea Research Institute of Bioscience and Biotechnology Research Initiative Program.

Author contributions

Conceptualization: SJK, WKL. Formal analysis: WKL. Funding acquisition: SJK. Supervision: SJK. Visualization: WKL. Writing - original draft: WKL. Writing - review and editing: SJK, WKL.

Author ORCIDs

Won-Kyung Lee https://orcid.org/0000-0001-7283-298X
Se-Joo Kim https://orcid.org/0000-0003-1653-072X

Data availability

All of the data that support the findings of this study are available in the main text or Supplementary Information.

References

Chen C, Copley JT, Linse K, Rogers AD (2015) Low connectivity between 'scaly-foot gastropod' (Mollusca: Peltospiridae) populations at hydrothermal vents on the Southwest Indian Ridge and the Central Indian Ridge. Organisms Diversity & Evolution 15: 663–670. https://doi.org/10.1007/s13127-015-0224-8

Darriba D, Taboada GL, Doallo Rn, Posada D (2012) jModelTest 2: more models, new heuristics and high-performance computing. Nature Methods 9: 772. https://doi.org/10.1038/nmeth.2109

Edler D, Klein J, Antonelli A, Silvestro D (2021) raxmlGUI 2.0: a graphical interface and toolkit for phylogenetic analyses using RAxML. Methods in Ecology and Evolution 12: 373–377. https://doi.org/10.1111/2041-210X.13512

Gamo T, Chiba H, Yamanaka T, Okudaira T, Hashimoto J, Tsuchida S, Ishibashi J-i, Kataoka S, Tsunogai U, Okamura K (2001) Chemical characteristics of newly discovered black smoker fluids and associated hydrothermal plumes at the Rodriguez Triple Junction, Central Indian Ridge. Earth and Planetary Science Letters 193: 371–379. https://doi.org/10.1016/S0012-821X(01)00511-8

Han Y, Zhou Y, Chen C, Wang Y (2023) Diversity and biogeography of scale worms in the subfamily Lepidonotopodinae (Annelida: Polynoidae) from Indian Ocean hydrothermal vents with descriptions of four new species. Zoological Journal of the Linnean Society 201: 290–304. https://doi.org/10.1093/zoolinnean/zlad140

Jang S-J, Cho S-Y, Li C, Zhou Y, Wang H, Sun J, Patra AK, Won Y-J (2023) Geographical subdivision of *Alviniconcha* snail populations in the Indian Ocean hydrothermal vent regions. Frontiers in Marine Science 10: 1139190. https://doi.org/10.3389/fmars.2023.1139190

Jimi N, Hookabe N, Moritaki T, Kimura T, Imura S (2021) First evidence of male dwarfism in scale worms: A new species of Polynoidae (Annelida) from hermit crab and molluscan shells. Journal of Zoological Systematics and Evolutionary Research 59: 801–818. https://doi.org/10.1111/jzs.12463

Jollivet D, Empis A, Baker M, Hourdez S, Comtet T, Jouin-Toulmond C, Desbruyeres D, Tyler P (2000) Reproductive biology, sexual dimorphism, and population structure of the deep sea hydrothermal vent scale-worm, *Branchipolynoe seepensis* (Polychaeta: Polynoidae). Journal of the Marine Biological Association of the United Kingdom 80: 55–68. https://doi.org/10.1017/S0025315499001563

Lee W-K, Lee GH, Ju S-J, Kim S-J (2021) Additional Records of the Hydrothermal Vent Scale Worm *Branchinotogluma segonzaci* (Polynoidae: Lepidonotopodinae) from the North Fiji Basin and Tonga Arc. Animal Systematics, Evolution and Diversity 37: 273–279. https://doi.org/10.5635/ASED.2021.37.4.027

Palumbi SR (1996) Nucleic Acids II: Polymerase Chain Reaction. In: Hillis D, Moritz C, Mable B (Eds) Molecular Systematic, 2nd edn. Sinauer Associates, Inc., Sunderland, 205–247.

Palumbi SR, Martin AP, Romano SL, McMillan WO, Stice L, Grabowski G (1991) The Simple Fool's Guide to PCR. Dept. of Zoology, University of Hawaii, Honolulu.

Perez Mv, Sun J, Xu Q, Qian P-Y (2021) Structure and connectivity of hydrothermal vent communities along the mid-ocean ridges in the West Indian Ocean: a review. Frontiers in Marine Science 8: 744874. https://doi.org/10.3389/fmars.2021.744874

Slatkin M (1987) Gene flow and the geographic structure of natural populations. Science 236: 787–792. https://doi.org/10.1126/science.3576198

Sun J, Zhou Y, Chen C, Kwan YH, Sun Y, Wang X, Yang L, Zhang R, Wei T, Yang Y (2020) Nearest vent, dearest friend: biodiversity of Tiancheng vent field reveals cross-ridge similarities in the Indian Ocean. Royal Society Open Science 7: 200110. https://doi.org/10.1098/rsos.200110

Tamura K, Stecher G, Kumar S (2021) MEGA11: Molecular Evolutionary Genetics Analysis version 11. Molecular Biology and Evolution 38: 3022–3027. https://doi.org/10.1093/molbev/msab120

Taylor M, Roterman C (2017) Invertebrate population genetics across Earth's largest habitat: The deep-sea floor. Molecular Ecology 26: 4872–4896. https://doi.org/10.1111/mec.14237

Van Dover CL, Trask J, Gross J, Knowlton A (1999) Reproductive biology of free-living and commensal polynoid polychaetes at the Lucky Strike hydrothermal vent field (Mid-Atlantic Ridge). Marine Ecology Progress Series 181: 201–214. https://doi.org/10.3354/meps181201

Vrijenhoek RC (2010) Genetic diversity and connectivity of deep-sea hydrothermal vent metapopulations. Molecular Ecology 19: 4391–4411. https://doi.org/10.1111/j.1365-294X.2010.04789.x

Wu X, Zhan Z, Xu K (2019) Two new and two rarely known species of *Branchinotogluma* (Annelida: Polynoidae) from deep-sea hydrothermal vents of the Manus Back-

Arc basin, with remarks on the diversity and biogeography of vent polynoids. Deep Sea Research Part I: Oceanographic Research Papers 149: 103051. https://doi.org/10.1016/j.dsr.2019.05.011

Wu X, Zhen W, Kou Q, Xu K (2023) Reevaluation of the systematic status of Branchinotogluma (Annelida, Polynoidae), with the establishment of two new species. Journal of Zoological Systematics and Evolutionary Research 2023: 1490800. https://doi.org/10.1155/2023/1490800

Zhang Y, Chen C, Qiu JW (2018) Sexually dimorphic scale worms (Annelida: Polynoidae) from hydrothermal vents in the Okinawa Trough: two new species and two new sex morphs. Frontiers in Marine Science 5: 112. https://doi.org/10.3389/fmars.2018.00112

Zhou Y, Wang Y, Zhang D, Wang C (2018) *Branchinotogluma bipapillata* n. sp., a new branchiate scale worm (Annelida: Polynoidae) from two hydrothermal fields on the Southwest Indian Ridge. Zootaxa 4482: 527–540. https://doi.org/10.11646/zootaxa.4482.3.5

Zhou Y, Chen C, Zhang D, Wang Y, Watanabe HK, Sun J, Bissessur D, Zhang R, Han Y, Sun D (2022) Delineating biogeographic regions in Indian Ocean deep-sea vents and implications for conservation. Diversity and Distributions 28: 2858–2870. https://doi.org/10.1111/ddi.13535

Supplementary material 1

Supplementary information

Authors: Won-Kyung Lee, Se-Joo Kim

Data type: docx

Explanation note: **table S1.** Sample information and accession numbers of the *Branchinotogluma* species used in this study (new sequences are highlighted in bold). **table S2.** Interspecific divergence (%) of mitochondrial *CO1* (below left) and 16S (upper right) genes of *Branchinotogluma* species. Mean intraspecific *CO1* distances are displayed in bold along the diagonal.

Copyright notice: This dataset is made available under the Open Database License (http://opendatacommons.org/licenses/odbl/1.0/). The Open Database License (ODbL) is a license agreement intended to allow users to freely share, modify, and use this Dataset while maintaining this same freedom for others, provided that the original source and author(s) are credited.

Link: https://doi.org/10.3897/zookeys.1215.129623.suppl1